Graphene-derivates containing responsive nanocomposite polymer gels: Effect of concentration and surface chemistry of the nanoparticles

Barbara Berke[1,2], László Sós[1], Virág Bérczes[1], Attila Domján[3], Lionel Porcar[2], Orsolya Czakkel[2*], Krisztina László[1]

[1]Department of Physical Chemistry and Materials Science, Budapest University of Technology and Economics, 1521, Budapest, Hungary

[2]Institute Laue Langevin, CS 20156, F – 38042 Grenoble Cedex 9, France

[3]NMR Research Group, Institute of Organic Chemistry, Research Centre for Natural Sciences, Hungarian Academy of Sciences, H-1117 Budapest, Magyar tudósok krt. 2, Hungary

*corresponding author; czakkelo@ill.fr

Abstract

Reduced graphene oxide (RGO) containing composite hydrogels, based on poly(*N*-isopropylacrylamide) (PNIPA) were prepared by two different methods: i) by incorporating RGO directly into the polymer matrix; ii) applying a post-synthesis reduction of the graphene-oxide (GO) already incorporated into the polymer. The samples were compared by various microscopic (small angle neutron scattering, differential scanning calorimetry, ^{1}H NMR spectroscopy, thermogravimetry) and macroscopic (kinetic and equilibrium swelling properties and mechanical testing) techniques. Results from microscopic and macroscopic measurements show that the dispersity of the nanoparticles as well as their interaction with the polymer chains are influenced by their surface chemistry. Incorporation of nanoparticles limits the shrinkage and slows down the kinetics of the thermal response. Both thermogravimetric and solid-state ^{1}H NMR measurements confirmed strong polymer – nanoparticle interaction when hydrophilic GO was used in the synthesis. In these cases, the slow thermal response may be explained by the decrease of the free volume inside the nanocomposite matrix caused by a hypernodal structure. Our results imply that both the chemistry and the concentration of incorporated graphene derivatives are promising in tuning the thermal responsivity of PNIPA.

Keywords: reduced graphene oxide; PNIPA; SANS; NMR spectroscopy; kinetics

1. Introduction

Responsive hydrogels are in the focus of scientific attention in the last few decades owing to their numerous beneficial properties like high water content [1,2] and relatively good deformability. Moreover, thanks to the physiochemical similarity of their network to the native extracellular matrix they are potentially biocompatible. Their responsiveness originates from a reversible volume phase transition (VPT) that can be triggered by changes in certain environmental conditions [3,4] like composition [5] or pH [6] of the swelling medium,

temperature [7], electromagnetic field [8], etc. This makes them very attractive for example in drug delivery [9,10], or as sensors [11], actuators [12,13], microvalves [14]. Poly(*N*-isopropylacrylamide) (PNIPA) is one of the most popular temperature sensitive responsive hydrogel, owing to its peculiar volume phase transition temperature (VPTT) that is at ~34 °C, close to the temperature of the human body [9,15]. Despite the above mentioned advantages hydrogels have several limitations as well (e.g. poor mechanical strength). Carbon nanoparticles (CNP) are widely used for strengthening in polymer nanocomposites. Recently they also got into the focus of interest as components of polymer *hydrogel* nanocomposites, as the CNPs may act not only as reinforcing agents, but may also provide new or modified sensitivity to these complex systems.

Graphene has many specific properties (e.g. excellent heat and electrical conductivity or light sensitivity) which would be beneficial, but its hydrophobicity hinders strongly the use in hydrogels. On the contrary, graphene oxide (GO), which is a damaged graphene layer, decorated with vacations and oxygen containing functional groups, forms stable aqueous suspension. However, due to the corrupted sp^2 structure, its properties are far from those of graphene. Several chemical and physical routes are available for partially restoring the honeycomb structure and removing the functional groups [16]. The resulted reduced graphene oxide (RGO) can have great potential in hydrogel nanocomposites as its properties are close to that of the graphene, but its hydrophobicity is decreased [17].

Nowadays GO containing systems are in the focus of attention [18–21] and few attempts have been already made to prepare various RGO containing composite materials [22–26] as well. In practice, though, the decreased hydrophilicity of RGO (with respect to GO) complicates the preparation of stable aqueous suspensions and consequently causing inhomogeneous distribution of RGO in the composite [27]. If the synthesis procedure of the gel is not too sensitive for the environment, in situ reduction methods (i.e. reduction agent added to the initial precursor mixture) may be used [28,29]. An effective way to make RGO containing gel composites is to reduce the already incorporated GO inside the gel matrix [30,31], however the circumstances of the reduction (e.g. reducing agent, temperature) should be chosen with great care in order not to affect the physical/chemical properties of the gel.

The preparation of RGO containing, PNIPA based, temperature sensitive hydrogels is challenging. As the free radical polymerisation of NIPA is extremely sensitive to the reaction circumstances, the application of even the mildest reducing agent for an eventual in-situ reduction of GO is excluded. On the other hand, incorporation of RGO nanoparticles into the gel matrix is limited owing to the above mentioned reduced hydrophilicity of RGO. In our paper we show that a treatment with L-ascorbic acid solution, which was proven to be an efficient and environmental friendly reducing agent of GO [32,33], can be used as a post treatment of GO containing PNIPA hydrogel nanocomposites to reduce GO within the gel matrix. Here we compare the microscopic and macroscopic character of differently prepared GO and RGO containing nanocomposite systems, based on results from small-angle neutron scattering (SANS), kinetic and equilibrium swelling properties, macroscopical mechanical tests and differential scanning calorimetry (DSC) measurements. Our results from solid state ^{1}H NMR spectroscopy and thermal analysis help to shed light on the interactions that are formed between the nanoparticles and the gel matrix.

2. Materials and methods

Nanoparticle synthesis

Graphene oxide (GO) was obtained by the improved Hummer's method [34] from natural graphite (originated from Madagascar). The GO content of the light brown suspension was ~1 w/w%. The C/O ratio of this GO, determined by XPS, was 1.8.

To prepare RGO we modified the method of Fernandez-Merino et al. [33]. The dry nanoparticles were suspended in L-ascorbic acid (AA) solution in the presence of NH_3 at 20 °C. In the reaction mixture the concentration of the GO, AA and NH_3 was 1 mg×ml^{-1}; 20 mmol×dm^{-3} and 1.1 mol×dm^{-3}, respectively. After 1 week of soaking the nanoparticles were purified by multiple washing and filtering steps. The resulted RGO was then dried and later stored in a desiccator at ambient temperature. The C/O ratio of RGO, determined by XPS, was 3.6. For nanocomposite gel preparation, RGO nanoparticles were re-suspended in water by ultrasonication.

Gel synthesis

The pure PNIPA were synthesised from *N*-isopropylacrylamide (NIPA) monomer (Tokyo Chemical Industry, Japan) and *N,N'*-methylenebisacrylamide (BA) cross-linker (Sigma Aldrich) in aqueous medium at 20 °C by free radical polymerization, as reported previously [35,36]

GO and RGO containing nanocomposite gels (GO@PNIPA and RGO@PNIPA, respectively) were prepared according to the method described earlier [35,36]. The GO loading was varied between 0 and 25 mg GO/g monomer, whereas the highest reachable concentration of RGO was only 11 mg/g monomer due to its poor dispersibility.

The post-reduction treatment of GO@PNIPA gels were made by soaking dried samples in the AA media (composition is identical as used for GO nanoparticle reduction, described above) for 1 week at 20 °C. The ratio of the solid (S) and liquid (L) phases was kept constant (S/L=0.012).

In all cases 2 mm thick films and 10 x10 mm isometric cylinders were prepared. All chemicals were used as received, except NIPA, which was recrystallized from a toluene-hexane mixture. Doubly distilled water was used for the synthesis, purification and measurements, unless stated differently.

The nomenclature of the prepared samples is given in Table 1.

Table 1. Nomenclature of the presented samples

Sample name	Nanoparticle content (mg/g monomer)	Reduction of GO
PNIPA	-	-
GO2.5@PNIPA	2.5	-
GO5@PNIPA	5	-
GO10@PNIPA	10	-
GO15@PNIPA	15	-
GO25@PNIPA	25	-
(PNIPA)R	-	inside the gel matrix
(GO2.5@PNIPA)R	2.5	inside the gel matrix
(GO5@PNIPA)R	5	inside the gel matrix
(GO10@PNIPA)R	10	inside the gel matrix
(GO15@PNIPA)R	15	inside the gel matrix
(GO25@PNIPA)R	25	inside the gel matrix
RGO3@PNIPA	3	prior to gel synthesis
RGO11@PNIPA	11	prior to gel synthesis

Methods

Equilibrium swelling degree of the samples was measured on dried gel disks with a diameter of 7 mm, cut from the 2 mm thick film. After 1 week in pure water at 20.0±0.2 °C the equilibrium swelling degree was determined as m/m_0, where m and m_0 are the mass of the swollen and dry samples, respectively.

Elastic modulus of the fully swollen samples was measured on isometric gel cylinders with an INSTRON 5543 mechanical testing equipment at ambient temperature. Samples were compressed by 10% of their initial height in steps of 0.1 mm with a relaxation time of 4×4 s and force threshold of 300 N. No barrel distortion was observed [37].
The reported equilibrium swelling degree and elastic modulus data are result of averaging 3 parallel measurements.

XRD measurements were carried out on dry gel disks. An X'pert Pro MPD (PANanalytical) multi-purpose powder X-ray diffractometer were used.

SANS measurements were performed on the D22 small angle instrument at the Institut Laue-Langevin. The gels were swollen in D_2O in order to enhance the scattering contrast between the polymer and the matrix, and to minimize the incoherent background scattering. The incident neutron wavelength was 6 Å. Two sample-detector distances (17 m and 2 m) were used to cover a Q-range of 0.004 – 0.5 $Å^{-1}$. Raw SANS data were corrected for the empty cell, dark counts, sample thickness and detector efficiency. The corrected scattering data were normalized by the incident beam flux to obtain the scattered intensity in absolute units. Data reduction was done with the GRASansP v.7.04 program. In case of nanocomposite samples the weak signal from the corresponding nanoparticle suspension has been subtracted in order to obtain the pure polymer signal.

Solid-state magic angle spinning (MAS) spectra of samples were recorded on a Varian NMR system operating at a ^{1}H frequency of 400 MHz with a Chemagnetics 3.2 mm narrow-bore double resonance T3 probe in. The spinning rate of the rotor was 8 kHz in all cases. For the one-dimensional ^{13}C CP MAS (cross-polarization magic angle) and DE (direct excitation) spectra SPINAL-64 decoupling with 83 kHz of strength was used. The nanoparticles and the composite samples were measured with DE with 120 s of recycle delay. The CP MAS build up curves were recorded in the range of 0-4 ms with a recycle delay of 5 s, which is 5 times larger thanT_{1H}.

Thermal analysis (TA) was carried out on an STA6000 instrument (PerkinElmer) in high-purity (99.9995%) nitrogen with the flow rate of 20 mL×min^{-1}. Prior to the experiments gel samples were air-dried, ground in an agate mortar and stored in a desiccator over silica gel. Samples of about 10 mg were heated from 30 to 650 °C in nitrogen atmosphere with a scanning rate of 10 C min^{-1}. The thermogravimetric (TG) curves were recorded. For the RGO and GO nanoparticles a slower scanning rate of 1.5 C min^{-1} was applied below 300 °C.

Scanning microcalorimetry measurements were made on finely ground samples in a MicroDSCIII apparatus (SETARAM). About 10 mg of dry gel were placed in contact with 500 µl of Millipore water and kept at 20 °C for 2 h to allow the gels to equilibrate. The samples were heated to 50 °C with a scanning rate of 0.03 °C/min. The instrument software was used to determine the peak position.

The kinetics of the temperature responsivity of the samples were studied on gel disks of 13 mm diameter (D_0) and 2 mm of thickness. The samples were first swollen in water at 20±0.2 °C to reach equilibrium, then plunged into a water bath of 50±1 °C. The thermal shock induced shrinkage was followed by measuring regularly the diameter D of the disks during 33 hours. Three parallel samples were measured at each case. Values of D were read in five positions for each sampling. Results are reported as $100 \times D/D_0$.

3. Results and discussion

The microscopic structure of the samples was explored by small angle neutron scattering (SANS) measurements [38] . As was shown earlier [36] SANS measurements can deliver structural information from the polymer matrix, whereas CNPs remain practically invisible. The corrected curves (typical examples are shown on Figure 1a) were fitted to the modified Ornstein-Zernike (OZ) expression [39,40] in the range of Q > 0.01 Å^{-1}. The deviation in the Q < 0.01 Å^{-1} region stems from the well-known concentration inhomogeneities due to cross-linking in gel networks [41] . In the OZ model the scattered intensity can be described by

$$I(Q) = \frac{I(0)}{1+(Q\xi)^n} + B \qquad (1)$$

where $I(0)$ and B are Q-independent constants, ξ is the static polymer–polymer correlation length and n is the fractal dimension of the polymer coils. As can be seen on Figure 1b, both the type and the concentration of the CNPs have pronounced effect on the correlation length ξ of the polymer matrix.

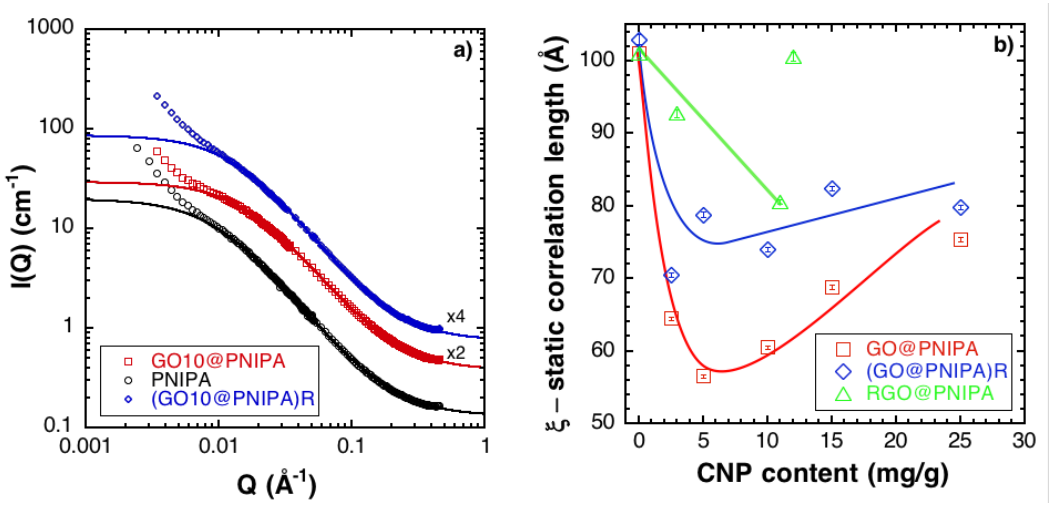

Figure 1: a) Representative SANS response curves (symbols) of nanocomposite systems with different CNPs. Solid lines are fits of Eq 1. Note that the curves are shifted vertically for clarity. b) Influence of CNP content on the static correlation lengths at 25 °C. Solid lines are guides to the eye.

Even the smallest amount of CNP present in the nanocomposites results in a significant drop of ξ. In chemical gels, ξ is usually interpreted as the size of cross-linked nods [42], and is inversely proportional to the cross-link density. In our previous work [36] we found, that at high GO content the architecture of the network is dominated by crosslink hypernodes and ξ is significantly smaller than in pure PNIPA gel. Here we present a detailed concentration study, which reveals that the effect of the incorporated CNPs is complex. In case of GO@PNIPA and (GO@PNIPA)R the increase in CNP concentration resulted in an increase in ξ as well. Nevertheless, even at the highest CNP concentration ξ remains significantly smaller than in the pure PNIPA. The increasing trend of ξ upon increasing CNP loading may indicate that at higher concentrations the GO nanoparticles sterically hinder each other, resulting a smaller effective concentration. As a consequence, they give rise to less hypernodes thus their structure modification effect is also smaller. Interesting to note, that XRD measurements excluded the formation of long-term reorganization of the nanosheets in the nanocomposites, so the decreased effective concentration cannot be explained by stacking of the GO sheets. After the post-reduction treatment ξ increased at all CNP concentrations (comparison of red squares and blue rhombi datasets on Figure 1b). On the other hand, no effect was observed in the pure CNP-free gel (red square and blue rhombi at 0 CNP concentration on Figure 1b) after the same treatment. The latter suggests that the pure polymer matrix is not affected by the reduction procedure, i.e. the chemical crosslinks are untouched. However, the change in ξ in the nanocomposite systems after the post-reduction treatment indicates that the hypernode structure of GO@PNIPA system was partially disrupted, possibly by breaking bonds between the nanoparticles and the polymer matrix. On the contrary to the other two cases, when RGO was directly incorporated into the polymer matrix ξ decreased upon concentration increase. The structure modification effect at the

lowest concentration is much less pronounced than in the other two cases, which is possibly related to aggregation of RGO even at low concentrations.

Beside the microscopic structure, the macroscopic properties of the nanocomposites are also significantly different. Similarly to earlier findings [35,36,43], the incorporation of GO effectively improved the mechanical properties and simultaneously decreased the swelling degree (Figure 2a and b). After the post-reduction treatment these properties remained almost unaffected. This may be because either the reinforcement is due to a simple mechanical effect (where surface chemistry and chemical interactions play no role); or, if there are chemical interactions between the GO and the polymer matrix, those interactions that determine the mechanical properties are unaffected by the applied treatment. On the contrary to GO, when RGO nanoparticles are incorporated directly to the PNIPA gel the mechanical and swelling properties of the nanocomposites remain practically unchanged. As RGO tends to form aggregates in aqueous media, its effective concentration within the gel matrix is much lower than the theoretical one, and in addition to that, it is not homogenously distributed (Figure 2c). This can explains the observed, very different behaviour of the RGO@PNIPA samples.

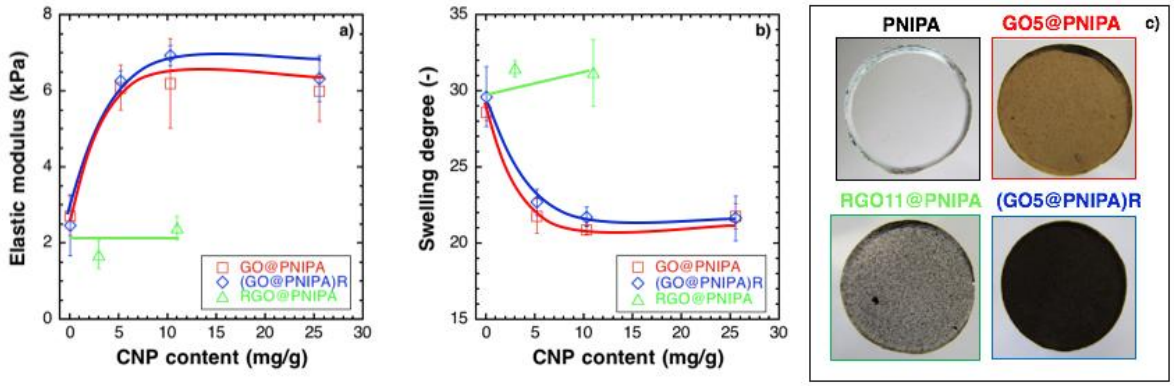

Figure 2: (a) Elastic moduli and (b) Swelling degree of composite gels. (c) Representative pictures of pure PNIPA and the different nanocomposites.

As was described above, both our SANS and macroscopic measurements suggest a strong interaction between the CNPs and the polymer matrix. A similar suggestion has been proposed earlier as well [25,43,44], however the nature of these interactions is still unrevealed. The possibilities are numerous, e.g. first order bonds with the oxygen containing functional groups or with the carbon lattice, secondary bonds (H-bonding) or entanglement of the polymer chains on the platelets [25,43,44]. To gain further knowledge, we have performed TA measurements which may help to shed light on this question. Although the shape of the TA curves was very similar for all the nanocomposite samples (Figure 3a), the obtained residual masses varied with the CNP type.

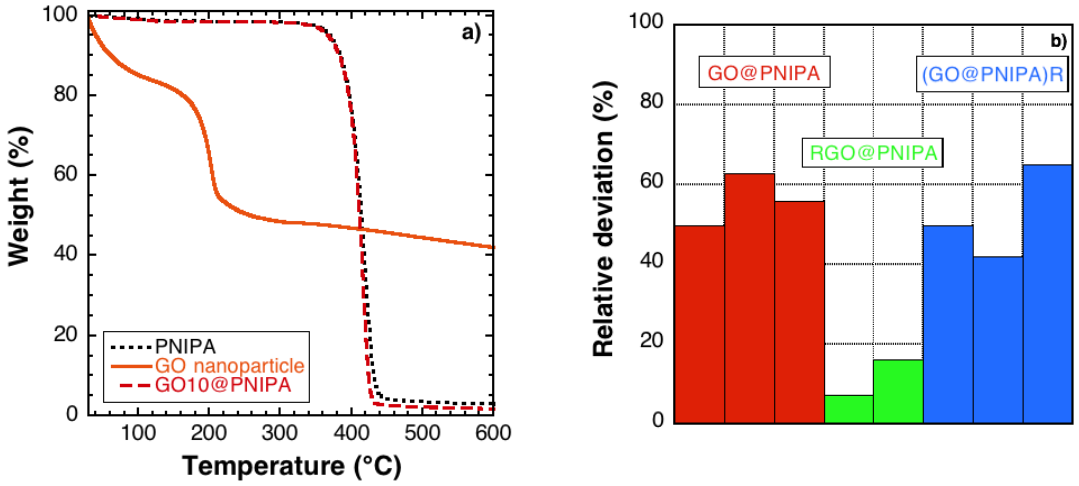

Figure 3: a) Thermograms of the pure PNIPA gel, GO nanoparticles and a GO-containing nanocomposite in N_2 atmosphere. b) Calculated difference between the theoretical (TRM) and experimental (ERM) values of the residual masses.

To quantify these differences, the theoretical residual mass (TRM) for independent decomposition was calculated from

$$TRM(\%) = c_{CNP} \cdot m_{CNP} + (100 - c_{CNP}) \cdot m_{PNIPA} \quad (2)$$

where c_{CNP} is the nanoparticle concentration in weight percentage, m_{CNP} and m_{PNIPA} are the residual masses at 600 °C for the nanoparticle and the pure PNIPA, respectively. TRM implies an independent decomposition, i.e. no interaction between CNP and the polymer matrix. The relative deviation of the experimental values (experimental residual mass, ERM) from TRM was calculated by

$$Relative\ deviation\ (\%) = \frac{ERM - TRM}{TRM} \cdot 100 \quad (3)$$

Comparing this relative deviation for the different CNPs significant differences can be observed (Figure 3b). The discrepancy in the case of GO containing gels was more than 50%. This suggests strong, possibly even covalent bonds between the GO sheets and the polymer chains. However, in our previous work we showed, that the effect of GO is more complex [36] than acting as a simple crosslinking agent. Post reduction had no significant effect on the deviation of ERM, suggesting that majority of the formed interactions between GO and the polymer matrix are not affected by the treatment. This is in line with the macroscopic observations. On the contrary, in RGO@PNIPA samples the relative deviation is significantly smaller (ERM is close to the theoretical value) indicating that the interactions between the RGO sheets and the polymer are much weaker.

As any future application of these systems rely on their responsiveness, the kinetics of an induced volume phase transition were also investigated. By following the shrinkage of the samples caused by a sudden increase of temperature from 20 to 50 °C it was found that

similarly to the macroscopic and microscopic structure, both the type and concentration of the CNPs have strong effect (Figure 4).

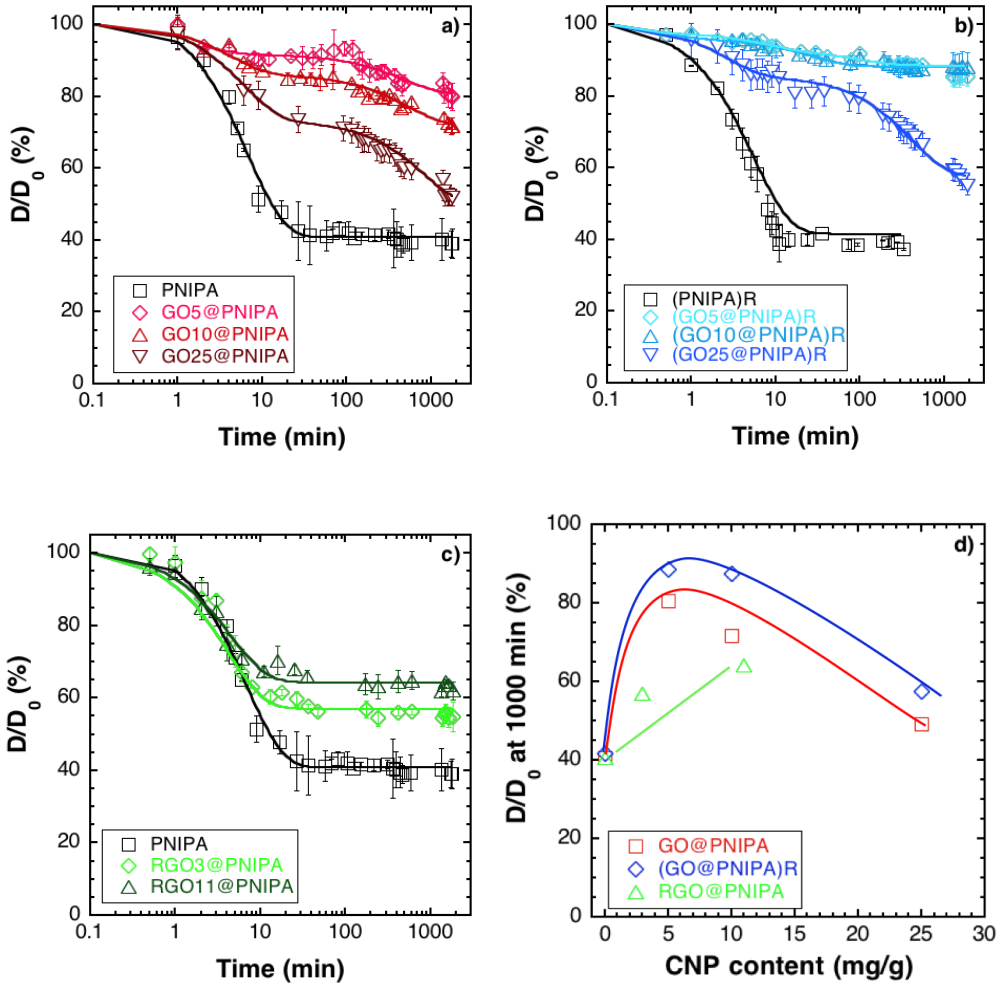

Figure 4: a-c) Kinetics of temperature jump (20 to 50 °C) induced shrinkage of pure and nanocomposite hydrogels. d) Relative diameter values 1000 minutes after the temperature jump. Solid lines are guides to the eye.

In all cases the shrinkage of the nanocomposite gel disks was less than that of the pure PNIPA gel after 1000 minutes, but the difference, as well as the shape of the shrinkage curves were different for the different systems. In cases where strong interaction is presumed between the CNPs and the polymer matrix (GO@PNIPA and (GO@PNIPA)R) the slower response may be explained by the decrease of the free volume inside the nanocomposite matrix [35,45] that is caused by the increasingly hypernode-like structure. The prolonged shrinkage of the samples suggests a complex process involving the deswelling of the gel matrix, the realignment of the CNP particles and the relaxation of the polymer chains [35,36].

Comparing the effect of the GO concentration on the kinetic behaviour of the systems (Figure 4d), a trend (i.e. the curves are going through an extreme value at medium GO loading) similar to what is observed in the structure (Figure 1b) can be observed. In other

words, at medium GO concentrations the nanocomposites can shrink less for a given temperature jump in a given time window, which can be explained by the structural differences of the systems. The ξ values are the smallest at medium GO concentrations meaning that the hypernode structure is the most pronounced. This causes a significant decrease in the free volume within the gel matrix, which can hinder the expulsion of water during the volume phase transition. The above mentioned description holds for the post-reduced systems ((GO@PNIPA)R) as well, suggesting that the decreased hydrophilicity of the RGO is still enough to provide the water with a way out of the polymer matrix. Nevertheless, the final deswelling ratios stayed slightly higher in these samples. Unlike the other two, RGO@PNIPA samples behave differently. Compared to pure PNIPA the timescale of the kinetic response is only slightly affected (Figure 4c), but the deswelling ratio remains higher after 1000 min. The influence of CNP concentration, however, is reversed, i.e. D/D_0 increases with increasing RGO concentration. This may be a result of the presence of large RGO aggregates in the system that may obstruct the adhesion of the PNIPA chains.

In general, the VPTT of the PNIPA-based gels can be tuned by changing its hydrophilic/hydrophobic balance, e.g., by copolimerization [46,47]. Our DSC measurements show no difference in the VPTT and the corresponding specific enthalpy (33.9±0.1 °C and 52±2 J/g, respectively) in the systems in Figure 5a. The unchanged specific enthalpy values suggest that the VPT is completed during the DSC conditions, which is not the case within the 1000 min period of the macroscopic thermal stress experiments. The lack of temperature depression can be explained by the low CNP concentration. Nevertheless, incorporation of CNP even in low amount alters the relaxation as revealed by the change of the peak widths.

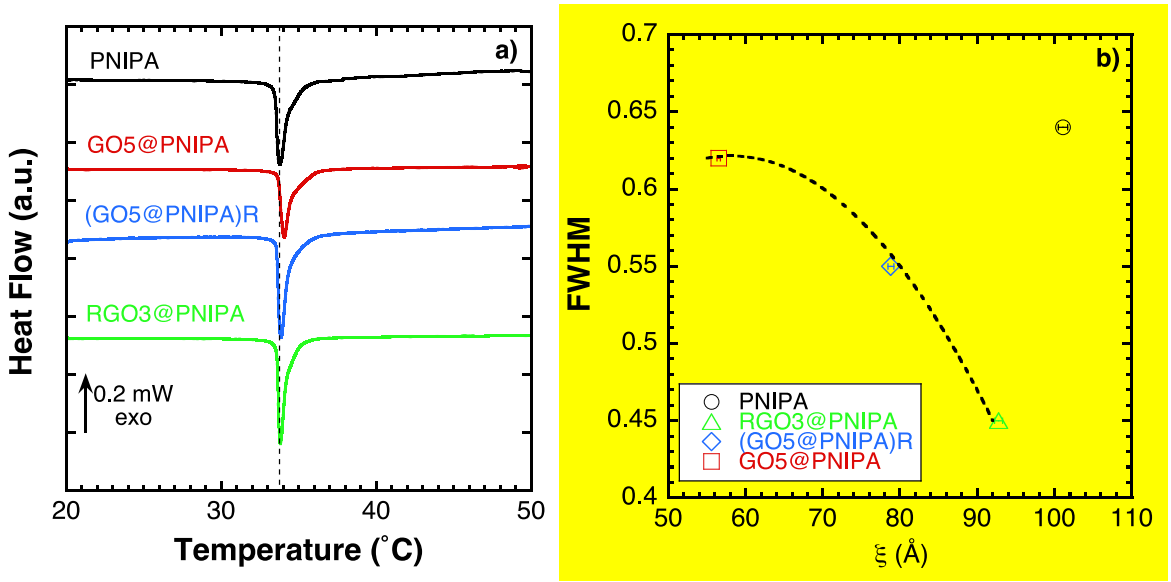

Figure 5: (a) Differential scanning calorimetry results of pure PNIPA and composite gels. Curves are shifted vertically for clarity. Broken vertical line indicates the peak position of pure PNIPA. (b) Full width at half maximum (FWHM) of the endothermic peaks from DSC as a function of the correlation length (ξ) of the polymer matrix.

This can be quantified by the full width at half maximum (FWHM), which also correlates well with the ξ values (determined from SANS) of the polymer matrix (Figure 5b) in the nanocomposite systems. As described above, the smaller ξ indicates a more developed hypernode structure, i.e., the reduced internal free volume can be responsible for the slower VPT in the nanocomposites.

Solid-state ^{1}H NMR investigations were carried out to get more information on the possible effects of GO/RGO on the properties of PNIPA composites. NMR spectroscopy is not only an important analytical method, but it is an effective technique that is widely used to characterize macromolecular systems, especially amorphous and mixed systems. Cross-polarization ^{13}C MAS spectra of the gel samples were found to be the same, no new signal can be observed. On the basis of this finding, we can exclude the formation of large number of new chemical bonds. Signals of GO or RGO cannot be identified because of their small amount in the samples and their broad signal structure.

Varying the contact time (*t*), in which the magnetization transfer occurs between the excited hydrogen atoms to the carbon atoms results the cross-polarization build-up curves. The shapes of the peak intensity (I(*t*)) vs *t* curves gives information on the proton environment of the carbon atoms and their mobility. The build-up curves have been fitted according to the I-I*-S model (Eq. 4) [48]

$$I(t) = I_0 \exp\left(-t/T_{1\rho}^{H}\right)\left[1 - \lambda \exp\left(-t/T_{df}\right) - (1-\lambda)\exp\left(-\frac{3}{2}t/T_{df}\right)\exp\left(-\frac{1}{2}t^2/T_2^2\right)\right] \quad (4)$$

where, I_0 corresponds to the plateau levels, $T_{1\rho}^{H}$ is the relaxation time constant of the ^{1}H in contact with the lattice in the rotating frame, T_{df} is the proton spin-diffusion constant, T_2 is the spin-spin relaxation time and $\lambda = 1/(n+1)$, where n is the number of ^{1}H in the spin system.

The build-up curves and the fitted parameters have been found to be the same for the isopropyl carbons, which suggests that the hydrophobic interactions between the isopropyl groups and the CNPs are negligible.

The build-up curves of the carbonyl carbons are nevertheless different in shape, as Figure 6 shows. Results of the fitting to Eq 4. are summarized in Table 2. The obtained $T_{1\rho}^{H}$ decreases at the GO@PNIPA and at the (GO@PNIPA)R in the same extent. This decrease indicates that the surrounding of the carbonyl group is more rigid then in pure PNIPA, which can be explained by strong interactions between PNIPA and GO nanoparticles. These interactions seem to be not affected by the post-reduction treatment. On the contrary, the increase of $T_{1\rho}^{H}$ in the RGO@PNIPA sample suggests an increased mobility in the environment of the carbonyl groups. Change of the T_{df} indicates changes also in the moeties of ^{1}H atoms in the environment of carbonyl atoms.

Table 2. Fitted parameters from the I-I*-S model to the cross-polarization build-up curves of the carbonyl carbon.

Sample	λ	T_{df} (ms)	$T_{1\rho}^{H}$ (ms)	T_2 (ms)	I_0 (a.u.)
PNIPA	0.75±0.05	2.0±0.1	13.9±0.1	0.1±0.01	62
GO@PNIPA	0.75±0.05	1.6±0.4	10.1±0.7	0.1±0.01	75
RGO@PNIPA	0.75±0.05	1.3±0.4	23.2±2.0	0.1±0.01	76
(GO@PNIPA)R	0.75±0.05	1.7±0.2	10.4±0.6	0.1±0.01	55

λ: = 1/(n+1), where n is the number of ^{1}H in the spin system; T_{df}: proton spin-diffusion constant; $T_{1\rho}^{H}$: relaxation time constant of the ^{1}H in contact with the lattice in the rotating frame; T_2: spin-spin relaxation time; I_0: plateau level

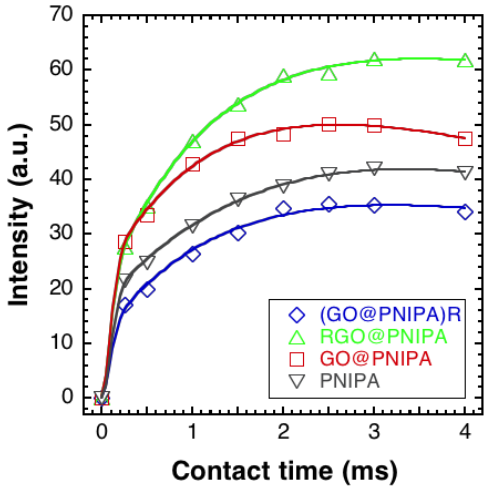

Figure 6: Solid-state NMR Cross- polarization build-up curves of carbonyl ^{13}C atoms. Solid lines are fits of Eq. 4 to the data points.

4. Conclusions

Reduced graphene oxide (RGO) containing composite hydrogels, based on poly(*N*-isopropylacrylamide) were prepared by two different methods: i) by incorporating RGO directly into the polymer matrix; ii) applying a post-reduction treatment on graphene oxide (GO) containing polymer nanocomposites. The effect of the carbon nanoparticle (CNP) concentration and the preparation method was investigated. Direct incorporation of RGO is strongly limited by its reduced hydrophilicity, i.e., only a smaller concentration and hardly uniform distribution were achieved. The more homogeneous distribution of the hydrophilic GO particles even at higher CNP content was conserved in the post-synthesis reduction. We found that the aggregation tendency of RGO reduced prior to the polymerisation resulted in small structural modification in the nanocomposites. The swelling and mechanical properties remained almost unchanged compared to the pure PNIPA gel. On the other hand, when GO

was reduced within the gel matrix both structural and macroscopic properties showed strong variation on the concentration of the CNPs. Thermogravimetric and ^{1}H NMR observations revealed strong interactions between GO and the polymer matrix, which are practically retained after the post-reduction treatment. Our results however show no clear evidence of covalent bonds. At the same time RGO interacts only weakly when incorporated directly into the gel. The vicinity of the PNIPA carbonyl groups is more rigid in the GO@PNIPA samples than in the pure PNIPA and this is not affected by the post-reduction. On the contrary, the mobility of the polymer in the same environment increases when RGO is directly incorporated into the polymer gel, implying a softening effect.

GO loading slows down the macroscopic shrinkage of the gel and the time scale of the response is extended. This behaviour is conserved after the post-reduction treatment. Direct incorporation of RGO into the polymer matrix hardly affects the timescale of the macroscopic response, but the observed shrinkage is smaller than in pure PNIPA gels.

The polymer-polymer correlation length (ξ), decreases upon CNP incorporation due to the hypernodal structure developing around the CNPs. As at higher concentration CNPs may sterically hinder each other, i.e. their effective concentration is smaller than the nominal, the effect is not proportional to the nominal concentration. Correlation between DSC results and the ξ values confirmed that the hypernodal structure may be responsible for the altered VPT.

Our results show that the incorporated graphene derivatives improve the mechanical properties of the PNIPA gel. Both their chemistry and their concentration are promising means for tuning the thermal responsivity broadening the application fields of such nanocomposite systems.

5. Acknowledgement

The authors are grateful to the ILL for providing beamtime on the D22 Instrument and thank to M. Jacques for his technical help during the experiment. The access to the PSCM laboratories and the assistance of D. Hess is acknowledged. The work was supported by the Hungarian Scientific Research Fund (OTKA) [grant number K115939]. A.D. acknowledges the support of the Bolyai Fellowship.

6. References

[1] N.K. Singh, D.S. Lee, In situ gelling pH and temperature-sensitive biodegradable block copolymer hydrogels for drug delivery, J. Control. Release. 193 (2014) 214–227. doi:10.1016/j.jconrel.2014.04.056.

[2] J. Kopecek, Hydrogel biomaterials: a smart future?, Biomaterials. 28 (2007) 5185–92. doi:10.1016/j.biomaterials.2007.07.044.

[3] J.H. Bradbury, M.D. Fenn, I. Gosney, the Change of Volume Associated With the Helix-Coil Transition in Poly-Gamma-Benzyl-L-Glutamate., J. Mol. Biol. 11 (1965) 137–140. doi:10.1016/S0022-2836(65)80179-6.

[4] M. Heskins, J.E. Guillet, Solution Properties of Poly(N-isopropylacrylamide), J. Macromol. Sci. Part A - Chem. 2 (1968) 1441–1455.

doi:10.1080/10601326808051910.

[5] T. Tanaka, Collapse of gels and the critical endpoint, Phys. Rev. Lett. 40 (1978) 820–823. doi:10.1103/PhysRevLett.40.820.

[6] J. Ricka, T. Tanaka, Swelling of ionic gels: quantitative performance of the Donnan theory, Macromolecules. 17 (1984) 2916–2921. doi:10.1021/ma00142a081.

[7] Y.H. Bae, T. Okano, S. Wan Kim, Temperature dependence of swelling of crosslinked poly(N,N′-alkyl substituted acrylamides) in water, J. Polym. Sci. Part B Polym. Phys. 28 (1990) 923–936. doi:10.1002/polb.1990.090280609.

[8] S. Reinicke, S. Döhler, S. Tea, M. Krekhova, R. Messing, A.M. Schmidt, H. Schmalz, Magneto-responsive hydrogels based on maghemite/triblock terpolymer hybrid micelles, Soft Matter. 6 (2010) 2760. doi:10.1039/c000943a.

[9] D.C. Coughlan, O.I. Corrigan, Drug-polymer interactions and their effect on thermoresponsive poly(N-isopropylacrylamide) drug delivery systems, Int. J. Pharm. 313 (2006) 163–174. doi:10.1016/j.ijpharm.2006.02.005.

[10] a. K. Bajpai, S.K. Shukla, S. Bhanu, S. Kankane, Responsive polymers in controlled drug delivery, Prog. Polym. Sci. 33 (2008) 1088–1118. doi:10.1016/j.progpolymsci.2008.07.005.

[11] A. Kumar, A. Srivastava, I.Y. Galaev, B. Mattiasson, Smart polymers: Physical forms and bioengineering applications, Prog. Polym. Sci. 32 (2007) 1205–1237. doi:10.1016/j.progpolymsci.2007.05.003.

[12] L. Ionov, Hydrogel-based actuators: possibilities and limitations, Mater. Today. 17 (2014) 494–503. doi:10.1016/j.mattod.2014.07.002.

[13] P. Kim, L.D. Zarzar, X. He, A. Grinthal, J. Aizenberg, Hydrogel-actuated integrated responsive systems (HAIRS): Moving towards adaptive materials, Curr. Opin. Solid State Mater. Sci. 15 (2011) 236–245. doi:10.1016/j.cossms.2011.05.004.

[14] S. Sugiura, K. Sumaru, K. Ohi, K. Hiroki, T. Takagi, T. Kanamori, Photoresponsive polymer gel microvalves controlled by local light irradiation, Sensors Actuators A Phys. 140 (2007) 176–184. doi:10.1016/j.sna.2007.06.024.

[15] K. Depa, A. Strachota, M. Šlouf, J. Hromádková, Fast temperature-responsive nanocomposite PNIPAM hydrogels with controlled pore wall thickness: Force and rate of T-response, Eur. Polym. J. 48 (2012) 1997–2007. doi:10.1016/j.eurpolymj.2012.09.007.

[16] S. Pei, H.-M. Cheng, The reduction of graphene oxide, Carbon N. Y. 50 (2012) 3210–3228. doi:10.1016/j.carbon.2011.11.010.

[17] S. Kim, Y. Yoo, H. Kim, E. Lee, J.Y. Lee, Reduction of graphene oxide/alginate composite hydrogels for enhanced adsorption of hydrophobic compounds, Nanotechnology. 26 (2015) 1–9. doi:10.1088/0957-4484/26/40/405602.

[18] D. Kim, H.S. Lee, J. Yoon, Highly bendable bilayer-type photo-actuators comprising of reduced graphene oxide dispersed in hydrogels, Sci. Rep. 6 (2016) 20921. doi:10.1038/srep20921.

[19] Z. Li, J. Shen, H. Ma, X. Lu, M. Shi, N. Li, M. Ye, Preparation and characterization of pH- and temperature-responsive hydrogels with surface-functionalized graphene oxide

as the crosslinker, Soft Matter. 8 (2012) 3139. doi:10.1039/c2sm07012j.

[20] C.-W. Lo, D. Zhu, H. Jiang, An infrared-light responsive graphene-oxide incorporated poly(N-isopropylacrylamide) hydrogel nanocomposite, Soft Matter. 7 (2011) 5604. doi:10.1039/c1sm00011j.

[21] X. Ma, Y. Li, W. Wang, Q. Ji, Y. Xia, Temperature-sensitive poly(N-isopropylacrylamide)/graphene oxide nanocomposite hydrogels by in situ polymerization with improved swelling capability and mechanical behavior, Eur. Polym. J. 49 (2013) 389–396. doi:10.1016/j.eurpolymj.2012.10.034.

[22] A. Flores, H.J. Salavagione, F. Ania, G. Martínez, G. Ellis, M.A. Gómez-Fatou, The overlooked role of reduced graphene oxide in the reinforcement of hydrophilic polymers, J. Mater. Chem. C. 3 (2015) 1177–1180. doi:10.1039/C4TC02425G.

[23] A. Gaffer, D. Aman, Preparation and Characterization of Conductive Polymer / Reduced Graphite Oxide (RGO) Composite via Miniemulsion Polymerization, 38 (2015) 35–39.

[24] S.B. Lee, S.M. Lee, N. Il Park, S. Lee, D. Chung, Preparation and characterization of conducting polymer nanocomposite with partially reduced graphene oxide, Synth. Met. 201 (2015) 61–66. doi:10.1016/j.synthmet.2015.01.021.

[25] Y. Zhuang, F. Yu, H. Chen, J. Zheng, jie ma, J. Chen, Alginate/graphene double-network nanocomposite hydrogel bead with low-swelling, enhanced mechanical property, and enhanced adsorption capacity, J. Mater. Chem. A. 4 (2016) 10885–10892. doi:10.1039/C6TA02738E.

[26] C. Teng, J. Qiao, J. Wang, L. Jiang, Y. Zhu, Hierarchical Layered Heterogeneous Graphene-poly(*N* -isopropylacrylamide)-clay Hydrogels with Superior Modulus, Strength, and Toughness, ACS Nano. (2015) acsnano.5b05120. doi:10.1021/acsnano.5b05120.

[27] A. GhavamiNejad, S. Hashmi, M. Vatankhah-Varnoosfaderani, F.J. Stadler, Effect of H2O and reduced graphene oxide on the structure and rheology of self-healing, stimuli responsive catecholic gels, Rheol. Acta. 55 (2016) 163–176. doi:10.1007/s00397-015-0906-3.

[28] A.J. Glover, M. Cai, K.R. Overdeep, D.E. Kranbuehl, H.C. Schniepp, In situ reduction of graphene oxide in polymers, Macromolecules. 44 (2011) 9821–9829. doi:10.1021/ma2008783.

[29] Y. Piao, B. Chen, One-pot synthesis and characterization of reduced graphene oxide–gelatin nanocomposite hydrogels, RSC Adv. 6 (2016) 6171–6181. doi:10.1039/c5ra20674j.

[30] S. Kim, Y. Yoo, H. Kim, E. Lee, J.Y. Lee, Reduction of graphene oxide/alginate composite hydrogels for enhanced adsorption of hydrophobic compounds, Nanotechnology. 26 (2015) 1–9. doi:10.1088/0957-4484/26/40/405602.

[31] L. Wu, M. Ohtani, M. Takata, A. Saeki, S. Seki, Y. Ishida, T. Aida, Magnetically induced anisotropic orientation of graphene oxide locked by in situ hydrogelation, ACS Nano. 8 (2014) 4640–4649. doi:10.1021/nn5003908.

[32] S. Pei, H.M. Cheng, The reduction of graphene oxide, Carbon N. Y. 50 (2012) 3210–3228. doi:10.1016/j.carbon.2011.11.010.

[33] M.J. Fernández-Merino, L. Guardia, J.I. Paredes, S. Villar-Rodil, P. Solís-Fernández, a. Martínez-Alonso, J.M.D. Tascón, Vitamin C is an ideal substitute for hydrazine in the reduction of graphene oxide suspensions, J. Phys. Chem. C. 114 (2010) 6426–6432. doi:10.1021/jp100603h.

[34] D.. Marcano, D.. Kosynkin, J.M. Berlin, A. Sinitskii, Z.Z. Sun, A. Slesarev, L.B. Alemany, W. Lu, J.M. Tour, Improved Synthesis of Graphene Oxide, Acs Nano (2010 Am. Chem. Soc. 4 (2010) 4806–4814. doi:10.1021/nn1006368.

[35] E. Manek, B. Berke, N. Miklósi, M. Sajbán, A. Domán, T. Fukuda, O. Czakkel, K. László, Thermal sensitivity of carbon nanotube and graphene oxide containing responsive hydrogels, Express Polym. Lett. 10 (2016) 710–720. doi:10.3144/expresspolymlett.2016.64.

[36] B. Berke, O. Czakkel, L. Porcar, E. Geissler, K. László, Static and dynamic behaviour of responsive graphene oxide - poly (N-isopropyl acrylamide) composite gels, Soft Matter. 12 (2016) 7166–7173. doi:10.1039/C6SM00666C.

[37] F. Horkay, M. Zrínyi, Studies on the Mechanical and Swelling Behavior of Polymer Networks Based on the Scaling Concept. 4. Extension of the Scaling Approach to Gels Swollen to Equilibrium in a Diluent of Arbitrary Activity, Macromolecules. 15 (1982) 1306–1310. doi:10.1021/ma00233a018.

[38] B. Berke, O. Czakkel, E. Geissler, K. László, L. Porcar, Structure of thermoresponsible nanocomposites below and above the volume phase transition temperature, 2016. doi:10.5291/ILL-DATA.9-12-446.

[39] L.S. Ornstein, F. Zernike, Accidental deviations of density and opalescence at the critical point of a single substance, Proc. Acad. Sci. Amsterdam. 17 (1914) 793–806.

[40] P. Pusey, W. van Meegen, Dynamic light scattering by non ergodic media, Phys. A1. 157 (1989) 705. doi:10.1016/0378-4371(89)90063-0.

[41] E. Geissler, F. Horkay, A.M. Hecht, Scattering from network polydispersity in polymer gels, Phys. Rev. Lett. 71 (1993) 645. doi:https://doi.org/10.1103/PhysRevLett.71.645.

[42] Z. Yang, Y. Hemar, L. Hilliou, E.P. Gilbert, D.J. Mcgillivray, M.A.K. Williams, S. Chaieb, Nonlinear Behavior of Gelatin Networks Reveals a Hierarchical Structure, (2016). doi:10.1021/acs.biomac.5b01538.

[43] K. Shi, Z. Liu, Y.-Y. Wei, W. Wang, X.-J. Ju, R. Xie, L.-Y. Chu, Near-infrared light-responsive poly(N-isopropylacrylamide)/graphene oxide nanocomposite hydrogels with ultrahigh tensibility, ACS Appl. Mater. Interfaces. (2015). doi:10.1021/acsami.5b08609.

[44] S. Hashmi, A. Ghavaminejad, J. Stadler, D. Wu, Soft Matter oxide and reduced graphene oxide with grafted, Soft Matter. 11 (2015) 1315–1325. doi:10.1039/C4SM02544J.

[45] W. Huang, J. Shen, N. Li, M. Ye, Study on a New Polymer/Graphene Oxide/Clay Double Network Hydrogel With Improved Response Rate and Mechanical Properties, Polym. Eng. Sci. (2015) 1361–1366. doi:10.1002/pen.24076.

[46] G. Kali, S. Vavra, K. László, B. Iván, Thermally responsive amphiphilic conetworks and gels based on poly(N -isopropylacrylamide) and polyisobutylene, Macromolecules. 46 (2013) 5337–5344. doi:10.1021/ma400535r.

[47] D. Schmaljohann, Thermo- and pH-responsive polymers in drug delivery, Adv. Drug Deliv. Rev. 58 (2006) 1655–1670. doi:10.1016/j.addr.2006.09.020.

[48] W. Kolodziejski, J. Klinowski, Kinetics of Cross-Polarization in Solid-State NMR : A Guide for Chemists, (2002) 613–628. doi:10.1021/cr000060n.